Polarized Raman spectroscopy of delta-BiB_3O_6 at 7–350 K

E. A. Strikina,[a]* A. S. Krylov,[a] A. S. Oreshonkov,[a,b] A. V. Cherepakhin[a,b] and A. N. Vtyurin[a,b]

BiB_3O_6 crystal has been characterized by Raman spectroscopy. Polarized low-frequency spectra have been obtained. Temperature measurements have been carried out in range 7–350 K. Raman spectra have been numerically simulated with LADY software package. The results of experiment confirmed the contribution of the Bi^{3+} ions and BO_4 groups in nonlinear optical properties of BiB_3O_6. The studied crystal is a promising medium for up- and down-Raman laser-frequency converters.

Keywords: orthorhombic bismuth triborate; lattice dynamics; laser medium

Introduction

Phase diagram of the Bi_2O_3-B_2O_3 system has been studied,[1–6] among them – crystals of bismuth triborate BiB_3O_6 have been synthesized. In recent years, high optical nonlinearity [6–9] of the crystal – an active medium for optical frequency transformation systems [10] attracted the particular interest of several scientific groups. For a long time, this composition was known to have only one α-phase [6–12]; however, in recent years, six new phases of BiB_3O_6 have been found.[13] Until lately, only α-phase was studied in detail.[1–14] The structure of the α-phase consists of chains of [BO_3] triangles and [BO_4] tetrahedrons in 1 : 2 ratio. [15–17] First principles simulations [18] of its electronic structure showed that optical nonlinearity is determined mainly by [BO_4] tetrahedrons.[19,20] Among other phases of BiB_3O_6, only γ and δ comprise [BO4] tetrahedrons exclusively; and centrosymmetric γ phase is of scant interest for nonlinear optics, while the structure of δ phase ($Pca2_1$, Z = 4) seems to be more attractive for such applications.[18–22] The structure and the photo of the δ-BiB_3O_6 are shown in Fig. 1, the experimental cell parameters and atomic coordinates can be taken from.[21]

The ab initio calculations of the phonon spectra, dielectric and elastic properties of the γ and δ modifications of the BiB_3O_6 crystal have been published in a previous study,[17,18] as well as the properties of the doped crystal.[19] The vibrational spectra and lattice dynamics calculations of δ-BiB_3O_6 were published earlier; the obtained spectra clearly exhibit significant LO–TO splitting for some polar modes and indicate that the contribution to the NLO response of δ-BiB_3O_6 may be associated both with the Bi^{3+} ions and BO_4 groups. This one also shows that δ-BiB_3O_6 is a promising medium for up- and down- Raman laser-frequency converters with the strongest lasing lines at 327, 124, and 99 cm^{-1}.[20] However, in earlier studies, the range of Raman spectra was limited down to 100 cm^{1} under ambient conditions. Heavy ions present in the structure allow assuming lower frequency modes in the Raman spectrum below 100 cm^{1}. Therefore, in this work, we attempt to fill a gap in the research and to study low frequency polarized Raman spectra of δ-BiB_3O_6 as well as to perform the low-temperature measurements, which remain unexplored.

Experimental

Samples for experiments were taken from the same crystallization as in a previous study.[21] The spectra in the backscattering geometry were recorded with Horiba Jobin Yvon T64000 spectrometer equipped with a liquid nitrogen cooled charge coupled device detection system in subtractive dispersion mode in 10 to 1600 cm^{1} range. Ar^{+} ion laser Spectra Physics Stabilite 2017 with λ° = 514.5 nm and power 3 mW on a sample was used as an excitation light source. The polarized experiments were carried out using incident laser beam focused on the sample by a 50× Olympus MPlan objective lens with a numerical aperture (NA) of 0.75. The scattered light was collected by the same objective lens in the backscattering geometry and analyzed through a polarizer and λ/2-plate. The spectroscopic measurements were performed in the subtractive dispersion mode to investigate the low-wavenumber spectra, which attained a low-wavenumber limit of 10 cm^{1} in the present setup. The deformation of the low-wavenumber spectral edge by an optical slit, which sometimes smears the true features of low-wavenumber spectra, was carefully eliminated by rigorous optical alignment. We use the standard notation [22] to describe the geometry of Raman scattering.

* Correspondence to: E. A. Strikina, Kirensky Institute of Physics, SB RAS, 660036, Krasnoyarsk, Russia.
E-mail: nas-nas@iph.krasn.ru

a Kirensky Institute of Physics, SB RAS, 660036, Krasnoyarsk, Russia

b Siberian Federal University, 660079, Krasnoyarsk, Russia

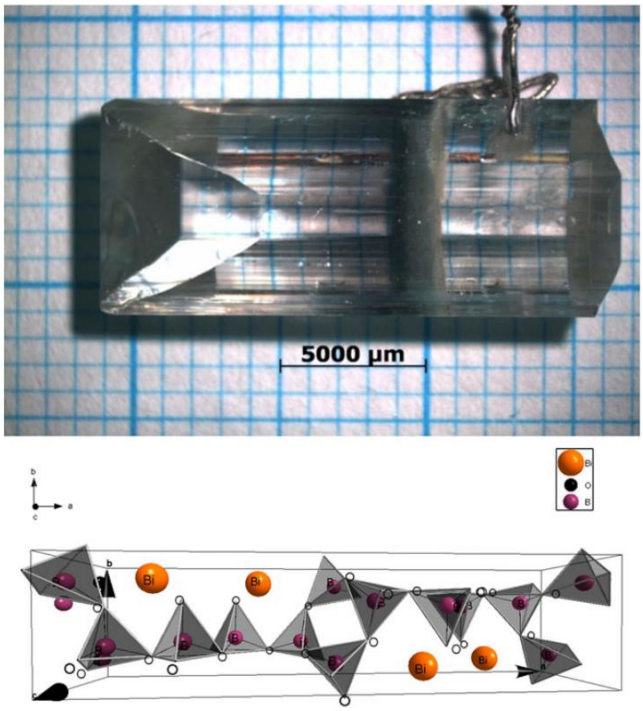

Figure 1. Top panel: The photo of the δ-BiB_3O_6, bottom panel: the crystal structure of δ-BiB_3O_6. [Colour figure can be viewed at wileyonlinelibrary. com]

The temperature studies were performed in a 6–350 K temperature range using an ARS CS204–X1.SS closed-cycle helium cryostat. The temperature was measured by calibrated LakeShore DT–6SD1.4 L silicon diode. The accuracy of temperature stabilization during spectra measurement was <0.2 K. The sample placed into an indium gasket was fixed on a coolant guide. The cryostat was evacuated to 10 ^{6} mbar.[23]

Results and discussion

Figure 2 presents the observed spectra down to 10 ^{1} cm at the room and 7 K temperatures for different polarizations.

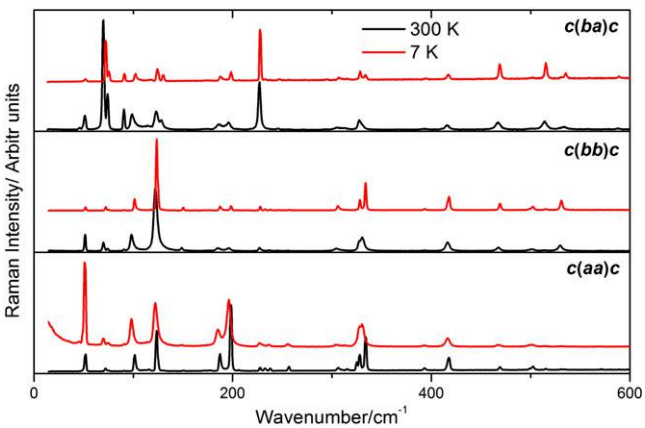

Figure 2. The Raman Spectra BiB_3O_6 on low wavelength and at the differences of temperatures. [Colour figure can be viewed at wileyonlinelibrary.com]

Vibrational representation of the $Pca2_1$ orthorhombic phase at Brillouin zone center of BiB_3O_6 crystal is (corresponding components of the Raman scattering tensor are given in brackets):

$$\Gamma_{vibr} ¼ 30A_1 þ 30A_2 þ 30B_1 þ 30B_2;$$

acoustic and optic modes:

$$\Gamma_{acoustic} ¼ A_1 þ B_1 þ B_2; \Gamma_{optic} ¼ 29A_1 þ 30A_2 þ 29B_1 þ 29B_2;$$

Raman and infrared active modes

$$\Gamma_{Raman} ¼ 29A_1ð aa; bb; ccÞ þ 30A_2ðab; baÞ þ 29B_1ðac; caÞ$$

$$þ29B_2ðbc; cbÞ;$$

$$\Gamma_{Infrared} ¼ 29A_1 þ 29B_1 þ 29B_2:$$

Temperature dependences of the lower wavenumber maxima positions were measured. Figure 3 shows a typical temperature dependence, as well as its slope (temperature derivative) near the room temperature. A complete list of observed line positions and such slopes is presented in Table 1.

As compared with data,[20] the most significant difference is several new lines at the lower frequency range, as well as slightly different positions of lower wavenumber lines. We suppose it to be due to temperature drifts of Raman lines and Bruker FT 100/S spectrometer lowpass filter that cut the low-wavenumber spectra.

Figure 4 shows lower frequency Raman spectra for all possible polarization directions where A1 and A2 modes are active (diagonal components of Raman tensor). In Fig. 4a and b, one can clearly see LO–TO splitting for A1 mode. Figure 5a and b presents Raman bands corresponding to B1 and B2 modes.

The vibrational spectrum of δ-BiB_3O_6 was simulated with LADY software.[24] Complete spectra of the δ-BiB_3O_6 crystal were obtained within the framework of a relatively common model of 'rigid-ions,' where the interatomic potential is considered as a sum of long-range Coulomb electrostatic interactions:

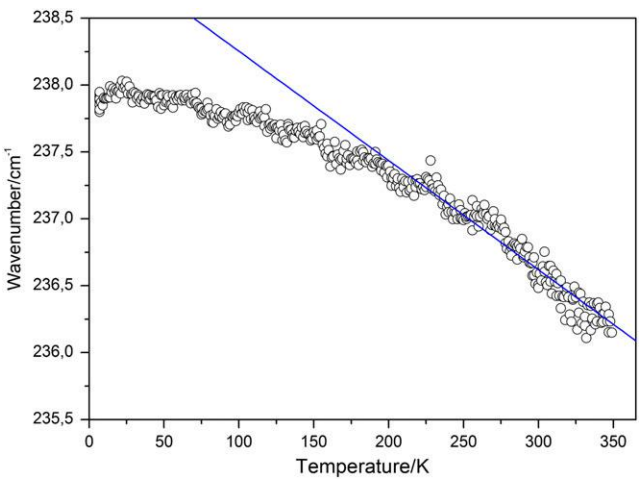

Figure 3. Typical temperature dependence of low-frequency line position. Line demonstrates a slope of temperature dependence near room temperature. [Colour figure can be viewed at wileyonlinelibrary.com]

Table 1. Positions (in cm $^{-1}$) and temperature slopes of the observed Raman lines

c(aa)c A_1 LO			c(ba)c A_2			c(bb)c A_1 LO		
ω, 300 K	[20]	$\frac{dw}{dt} \times 10^{-3}$	ω, 300 K	[20]	$\frac{d\omega}{dt} \times 10^{-3}$	ω, 300 K	[20]	$\frac{dw}{dt} \times 10^{-3}$
51 s	—	3.09	51 m	—	2.72	51 s	—	1.67
70 m	—	8.94	70s	—	9.9	70 m	—	9.22
75w	—	3.06	74 m	—	6.16	75w	—	5.8
98 s	—	11.6	91 m	—	1.98	91vw	—	1.03
—	109 m	—	99 m	108 m	12.63	98 s	—	11.58
115w	116w	*	115w	115sh	*	—	109	—
122 s	124 s	5.08	123 m	124 s	4.68	—	116	—
149w	150 w	9.13	128 m	—	8.72	122 s	124	5.04
185 m	170w	9.25	186w	170w	10.95	149w	150	6.46
196 s	195 s	11.19	191 m	—	11.54	185w	170	8.36
—	206w	—	196 m	196 s	0.011	196w	195	11.07
228w	228 s	5.01	—	205w	—	—	206	—
236vw	247w	9.1	227 s	228 m	5.3	227w	228	5.25
255vw	256w	5.6	233	—	*	236w	—	6.83
305vw	—	9.52	246w	246w	8.63	246w	247	5.99
313vw	314 m	9.1	305vw	255vw	10.81	255w	256	7.94
330 s	329 s	14.09	313vw	314 m	6.42	305w	314	4.95
393vw	395w	6.81	328 m	329 s	4.17	327 m	329	4.69
—	402vw	—	331 m	—	14.26	330 m	—	14.35
416 s	417 s	8.17	394w	394w	8.16	393 m	395	6.48
467vw	467 m	9.33	—	401vw	8.38	—	402	—
501vw	501w	8.53	416w	417 m	10.42	417 m	417	6.42
515vw	515w	*	467 m	467 m	9	467 m	465	5.75
530w	530 m	9.26	—	501w	9.56	502w	501	11.31
607w	607w	6.07	514 m	514w	6.59	514w	514	7.06
—	—	—	533w	530w	5.52	530 m	530	5.54
—	—	—	588w	—	—	—	607	—
—	—	—	607vw	607w	—	—	—	—

* we failed to calculate the slope for this maximum $\frac{dw}{dt}$, but we can observe it in the spectra. s, m, w, vw and sh denote strong, medium, weak, very weak and shoulder, respectively.

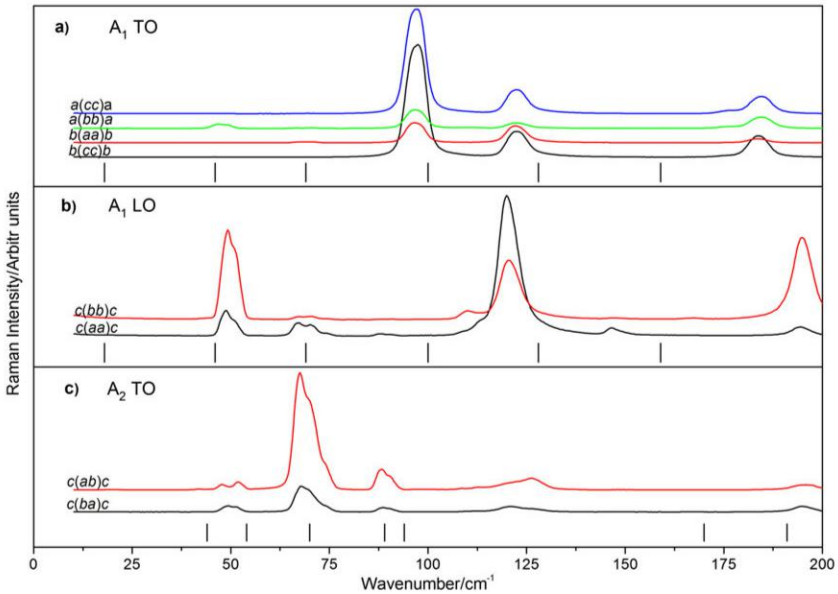

Figure 4. Raman spectra of the δ-BiB_3O_6 crystal at: a) a(cc)a, a(bb)a, b(aa)b, b(cc)b; b) c(bb)c, c(aa)c; c) c(ab)c, c(ba)c geometries. [Colour figure can be viewed at wileyonlinelibrary.com]

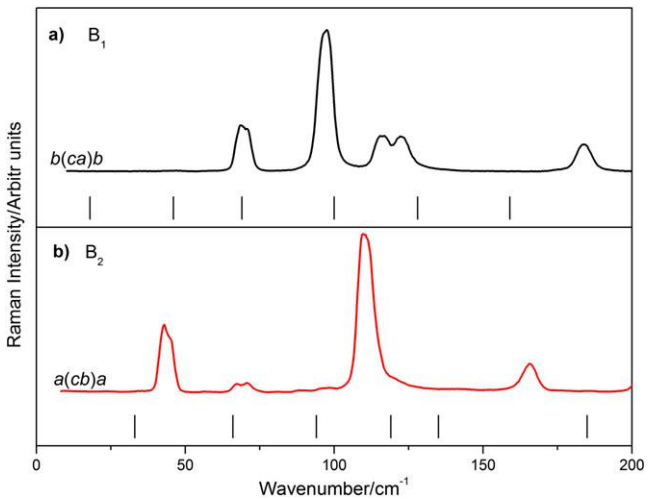

Figure 5. Raman spectra of the δ-BiB_3O_6 crystal at: a) b(ca)b; b) a(cb)a. [Colour figure can be viewed at wileyonlinelibrary.com]

$$V^{RIM}(r_{ij}) = \frac{1}{2}\sum_{i \neq j}\left(\frac{Z_i Z_j}{r_{ij}} + U(r_{ij})\right); \quad (1)$$

and the short-range interaction potential in Born–Mayer form:

$$U(r_{ij}) = \lambda \exp(-r_{ij}/\rho); \quad (2)$$

where r_{ij} is the interatomic distance, and λ and ρ are the parameters of the short-range pair interionic interactions. Resulting model parameters were obtained by minimization of residual values of the simulated and experimental Raman wavenumber using the Fletcher–Reeves method.[24–26] The values of λ, ρ and Z_{ij} are listed in Table 2. Calculated positions of Raman active modes are shown in Table 3 in comparison with experimental results. To build the model, we used atomic charges Z(e): Bi = 2.00, B = 1.80, O = 1.2333 while, Mirosław Maczka et al. used Z(e): Bi = 2.1, B = 1.5, O = 1.1.[20]

Only normal symmetric stretching ν_1 and antisymmetric stretching ν_3 vibrations should appear above 650 cm^{-1}[27] for the ideal BO_4 tetrahedron. However, taking into account the fact that the atoms in δ-BiB_3O_6 are in general positions, the B–O distances are different and BO_4 tetrahedrons interconnected to each other, these internal modes should be strongly distorted and split. For this reason, this higher frequency spectral region and the whole spectrum is rich of lines of BO_4 tetrahedra. Our simulations show that about 40 Raman active modes should appear above 650 cm^{1} at different polarization geometries. The vibrational spectrum of δ-BiB_3O_6 was simulated with LADY software.[24] Complete spectra of the δ-BiB_3O_6 crystal were obtained within the framework of a relatively common model of 'rigid-ions', where the interatomic potential is considered as a sum of long-range Coulomb electrostatic interactions:

Figure 6 shows line positions versus temperature dependences. No significant anomalies were found within the whole range of δ phase existence that demonstrates the stability of this phase.

Table 2. Parameters of the interatomic interaction potentials

Interactions	Radii of interaction, Å	λ, aJ/Å^2	ρ, Å
Bi–O	0–3.00	350.00	0.300
B1–O	0–1.50	321.60	0.210
B2–O	0–1.60	400.60	0.220
B3–O	0–1.60	345.30	0.199
O–O	0–3.00	242.80	0.245

Table 3. Experimental and calculated positions (cm ^{1}) of Raman lines for δ-BiB_3O_6 crystal

A_1			A_2		B_1		B_2	
exp.		calc.	exp.	calc.	exp.	calc.	exp.	calc.
TO	LO							
1116w	1097 m	1121	1076s	1153	—	1212	—	1278
1081w	1035w	1093	1037s	1119	1082 m	1132	1037s	1132
1031s	1007 m	979	1010 m	1090	1035w	1023	1010s	1029
996 m	975w	959	978sh	981	997 m	949	997 m	965
959 m	935w	908	944 m	945	955w	938	956sh	929
919 sh	907 m	894	905 m	912	919 s	910	936 s	905
864vw	865sh	789	864 m	805	897vw	854	880 s	892
807vw	783 s	752	784 m	755	863 s	803	784 m	786
783 s	727 m	721	728w	751	813w	749	727w	737
752w	650w	697	709 m	730	783 m	732	665 s	689
726vw	607 m	634	607w	648	753w	648	607 m	647
639w	530 m	598	558 m	606	727vw	618	515vw	623
606 m	515w	552	534 m	553	607 m	575	499vw	563
530w	502 m	510	514 s	529	578 s	533	468w	518
499 m	467w	490	501vw	511	531 s	504	415 m	483
467 m	416 m	447	466 s	490	515vw	497	393w	459
415 s	394w	428	417w	428	500w	432	327 s	442
393w	329 s	384	393vw	416	467 m	421	312 m	400
328 s	310vw	345	330 m	382	415 s	392	304 s	383
303 s	256 m	320	313vw	332	394 m	347	249w	338
272vw	244vw	274	255vw	310	327 m	319	226 m	307
228 m	235w	255	246w	262	304 m	299	204 m	280
186 s	225w	221	226 s	227	245 s	267	185 m	240
175sh	194 s	159	196 m	191	229 m	229	177w	185
122 s	165w	128	126 m	170	184 m	156	166 m	135
97 s	120 s	100	110w	94	123 s	116	123 m	119
71 s	88 m	69	89 s	89	116 s	89	112 s	94
67 m	69 s	46	68 s	70	97 s	76	98 m	66
46 s	49 s	18	51 m	54	71 s	55	69 m	35
—	—	—	49 m	44	68 s	—	45 s	—

s, m, w, vw and sh denote strong, medium, weak, very weak and shoulder, respectively.

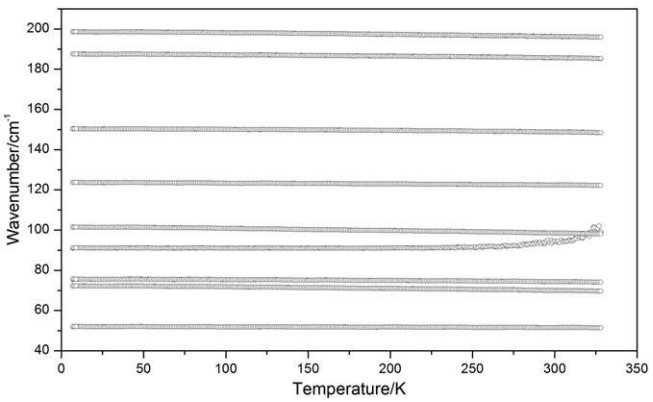

Figure 6. Line positions versus temperature dependences for δ-phase of BiB_3O_6 crystal.

Conclusions

The experimental Raman spectra of δ-BiB_3O_6 crystal for all possible polarizations have been found. The number of spectral lines is in agreement with the vibrational representation, polarization selection rules, and lattice dynamics simulations. The observed Raman bands are assigned to corresponding vibrational modes by the lattice dynamics simulations. No signs of phase instability have been found within the whole range of δ phase existence.

Acknowledgments

This study was partially supported by the Ministry of Education and Science of the Russian Federation, the Russian Foundation for Basic Research Grant '16-02-00102'.

References

[1] E. M. Levin, C. L. McDaniel, J. Am. Ceram. Soc. 1962, 45, 355.
[2] J. Z. Liebertz, Kristallogr. 1982, 158, 319.
[3] R. Fröhlich, L. Bohatý, J. Liebertz, Acta Crystallogr. C 1984, 40, 343.
[4] P. Becker, L. Bohatý, Cryst. Res. Technol. 2001, 11, 1175.
[5] B. Teng, Z. Wang, H. Jiang, X. Cheng, H. Liu, X. Hu, S. Dong, J. Wang, Z. Shao, J. Appl. Phys. 2002, 91, 3618.
[6] A. V. Cherepakhin, A. I. Zaitsev, A. S. Aleksandrovsky, A. V. Zamkov, Opt. Mater. 2012, 34, 790.
[7] R. Cong, T. Yang, Z. Lin, L. Bai, J. Jing, F. Liao, Y. Wang, J. Lin, J. Mater. Chem. 2012, 22, 17934.

[8] A. V. Egorysheva, V. I. Burkov, Y. F. Kargin, V. G. Plotnichenko, V. V. Koltashev, Crystall. Rep. 2005, 50, 127.
[9] D. Kasprowicz, T. Runka, M. Szybowicz, P. Ziobrowski, A. Majchrowski, E. Michalski, M. Drozdowski, Cryst. Res. Technol. 2005, 40, 459.
[10] R. Cong, J. Zhu, Y. Wang, T. Yang, F. Liao, C. Jin, J. Lin, Cryst. Eng. Comm. 2009, 11, 1971.
[11] R. Cong, T. Yang, Y. Wang, J. Lin, Inorg. Chem. 2013, 52, 7460.
[12] J. S. Knyrim, P. Becker, D. Johrendt, H. Huppertz, Angew. Chem. Int. Ed. 2006, 45, 8239.
[13] J. Yang, M. Dolg, J. Phys. Chem. B 2006, 110, 19254.
[14] E. A. Strikina, A. S. Krylov, A. S. Oreshonkov, A. N. Vtyurin, Ferroelectrics 2016, 501, 26.
[15] E. A. Strikina, A. S. Krylov, A. S. Oreshonkov, A. N. Vtyurin, O. A. Maximova, Mat. Sci. Eng. 2016, 155, 012029.
[16] J. S. Knyrim, P. Becker, D. Johrendt, H. Huppertz, Angew. Chem. Int. Ed. 2006, 45, 8239.
[17] M. S. Pavlovskii, A. S. Shinkorenko, V. I. Zinenko, Phys. Solid State. 2015, 57, 675.
[18] D. A. Ikonnikov, A. V. Malakhovskii, A. L. Sukhachev, A. I. Zaitsev, A. S. Aleksandrovsky, V. Jubera, Opt. Mater. 2012, 34, 1839.
[19] M. Maczka, L. Macalik, A. Majchrowski, J. Alloys Compd. 2013, 575, 86.
[20] A. S. Aleksandrovsky, A. D. Vasiliev, A. I. Zaitsev, A. V. Zamkov, J. Cryst. Growth 2008, 310, 4027.
[21] D. L. Rousseau, R. P. Bauman, S. P. S. Porto, J. Raman Spectrosc. 1981, 10, 253.
[22] A. S. Krylov, A. N. Vtyurin, A. S. Oreshonkov, V. N. Voronov, S. N. Krylova, J. Raman Spectrosc. 2013, 44, 763.
[23] M. B. Smirnov, V. Y. Kazimirov, LADY: software for lattice dynamics simulations, JINR Communications, Dubna, 2001.
[24] Y. V. Gerasimova, A. S. Oreshonkov, A. N. Vtyurin, A. A. Ivanenko, L. I. Isaenko, A. A. Ershov, Phys. Solid State. 2013, 55, 2331.
[25] Z. Xia, M. S. Molokeev, A. S. Oreshonkov, V. V. Atuchin, R.-S. Liu, C. Dong, Phys. Chem. Chem. Phys. 2014, 16, 5952.
[26] K. Nakamoto, Infrared and Raman Spectra of Inorganic and Coordination Compounds, Wiley, New York etc., 2009.